

Topological localisation and motility of active knots

A. Bonato,¹ D. Marenduzzo,¹ E. Orlandini,² and G. Negro¹

¹*SUPA, School of Physics and Astronomy, Edinburgh EH9 3FD, UK*

²*Department of Physics and Astronomy, University of Padova and Sezione INFN, Padova, Via Marzolo 8, I-35131 Padova, Italy*

Nonequilibrium active polymers provide a minimal framework to investigate biopolymers such as DNA and chromatin under the action of molecular motors. Here we study active ring polymers with controlled topology and show that knot type qualitatively determines their nonequilibrium behaviour. We find that activity induces opposite localisation responses in different topological families: torus knots systematically delocalise and inflate, whereas twist knots tighten and remain localised. We trace this divergent behaviour to the distinct symmetry properties of their tangent fields, which control the alignment of active forces along the chain. We show that topology also governs internal and emergent dynamics. Active torus knots behave as soft chiral self-propelled particles exhibiting persistent motion with a well-defined handedness fixed by their topological chirality. In contrast, achiral knots show no net handedness. The knot thus acts as a deformable topological quasiparticle whose morphology and propulsion are selected by topology. These results suggest potential routes toward programmable soft chiral particles with controllable morphology and emergent motility modes.

Biopolymers such as DNA and chromatin are kept out of equilibrium by, amongst others, the continual activity of polymerases [1–3], molecular motors such as condensin [4], and topological enzymes such as topoisomerases [5, 6]. Notwithstanding the critical role played by nonequilibrium phenomena, we still have a limited understanding of the effect of activity on polymer dynamics, and chromatin or DNA are still more commonly modelled as systems in thermal equilibrium.

Over the last decade, minimal models of active polymers have been proposed to explore how internal forcing reshapes polymer conformations and affects their dynamics [7–11]. Activity has been shown to induce a swollen-to-globule transition driven by persistent propulsion [7, 12], alter the mechanical response by softening the polymer via local kink formation [8], and significantly affect the probability of knot formation in linear diblock copolymers [13]. In ring geometries, activity can create additional spatiotemporal patterns, leading to rotating or coherently moving states that have no counterpart in equilibrium [14, 15]. More generally, active forcing breaks detailed balance [16] and can generate effective tensions, enhanced diffusion, and emergent alignment along the polymer backbone, fundamentally altering the physics of passive polymers [9]. For example, dense suspensions of active diblock ring polymers exhibit glassy behavior [17] that originates from a network of deadlocks [18]. Despite these advances, the role of topology in organizing nonequilibrium active polymers remains largely unexplored.

In this work, we study how topology constrains nonequilibrium polymer dynamics by focusing on active knotted rings or *active knots*. These may be viewed as soft topological quasi-particles, similarly to the way in which polymers can be coarse-grained into soft colloids [19]. In equilibrium, knots can perform anomalous diffusion along the polymer in which they are embedded [20] and adjust their size in response to external fields, confinement, or tension [21–24]. Importantly,

different knot families possess distinct symmetry properties [25]. Torus knots are generically chiral and admit globally ordered tangent fields, providing a potential quasiparticle analogue of active chiral rotors [26–28]; twist knots and achiral knots display instead very different symmetry constraints. This raises some natural questions: how does persistent active forcing reorganise stresses within a topologically constrained chain? Can topology alone encode dynamical chirality and control transport in an active polymer? Addressing these questions allows us to treat knots as deformable, self-organised active particles whose morphology and motility are selected by topology.

We show that activity fundamentally reshapes polymer knots in a topology-dependent manner. First, torus knots systematically delocalise as activity increases, expanding until the knotted region spans the entire ring. This behaviour contrasts sharply with the response of passive polymers under tension, where stretching typically promotes knot tightening and localisation [22, 23, 29, 30]. In contrast, twist knots and achiral knots become more localised under activity, forming compact entangled regions that slide along a weakly perturbed backbone. In both cases knots behave as mobile quasiparticles that reptate along the ring, with a timescale separation between the fast motion of beads through the knotted structure and the slower evolution of the knot’s global shape. Second, we find that topology controls emergent motility. Delocalised torus knots organise into coherently rotating structures that self-propel through space via helical trajectories reminiscent of chiral motility modes of chiral active droplets [31, 32]. The handedness of these trajectories is fixed by the knot’s topological chirality.

Model- We simulate active knots of $N_b = 64$ beads of size σ for various knot types π . This chain length was chosen to accommodate moderately complex knots while preventing the crumpling behavior observed in longer active knots [12]. We consider the trefoil knot 3_1 (which is both a twist and a torus knot), the twist knots $4_1, 5_2, 7_2$,

the torus knots 5_1 and 7_1 , and finally the knot 6_3 , which is neither a twist nor a torus knot. The non-equilibrium properties of the knots are studied via molecular dynamics simulations using LAMMPS [33], coupled to a custom modification implementing activity. Each bead in the knotted ring has a diameter σ and mass m , and evolves according to an overdamped Langevin equation with friction $\zeta = 1$ and temperature $T = 0.5$ in LJ units [34]. This sets a unit of time $\tau = \sigma\sqrt{m/2k_B T}$. The beads interact via a WCA potential, while two consecutive beads interact through a FENE potential. Chain stiffness is described via a bending (Kratky-Porod) potential. Knots are assigned an orientation, and activity is modelled as a constant force F_a pushing each bead tangentially to the backbone of the polymer. We consider forces in the interval $F_a \in [0, 10]$, in units of $2k_B T/\sigma$, which corresponds to Peclet number $Pe := F_a\sigma/k_B T \in [0, 20]$. For all the results presented we fixed the simulation time-step to $dt = 10^{-3}\tau$, equilibrated initial configurations for 300τ , and run the simulations for $9 \times 10^5\tau$ before collecting data and compute observables. More details are given in [34].

Activity induced knot tightening and delocalisation- To assess the effects of activity on equilibrated knotted rings, we look at the size and position of the knotted portion. This is done by using *KymoKnot* [35], which systematically computes the Alexander polynomial [25] on closed subarcs of each sampled configuration [36]. Remarkably, the behavior of the knotted portion strongly depends on the underlying topology: as the activity increases, the torus knots 5_1 (Fig. 1(a)-(d)) and 7_1 inflate and, at higher values of the active force, adopt quasi-ideal toroidal conformations, where the knotted region occupies the entire ring (Fig. 1(d) and Movie1) [37]. Conversely, activity causes the knotted portions of twist knots 5_2 (Fig. 1(b)-(e) and Movie2) 7_2 (Fig. 1(c)-(f)), and knot 6_3 , to tighten. The resulting conformations can be described as unknotted loops crowned by a sliding root that encapsulates the compact knotted region. Surprisingly, this steady state non-equilibrium structure resembles the conformations adopted by asymptotically long knots and links in the passive regime [38–40].

To quantify the effects of tightening and delocalisation, we computed the average size of the knotted region as a function of the Peclet number. As shown in Fig. 1g, increasing activity causes torus knots to expand beyond their size at equilibrium, whereas other knot types contract significantly. This difference in entanglement localization between torus and non-torus knots can be explained by monitoring the orientation of the knots while diffusing along their contour. When the activity is high, a knot tends to conform to its ideal shape [37], since it becomes effectively stiffer. Fig. 1(i) shows that activity directions are locally disordered in quasi-ideal twist knots but aligned with neighboring beads in torus knots. The polar order emerging in highly active torus knots, which makes them more stable toward big conformational changes, is quantified in Fig. 1(h), where we report the

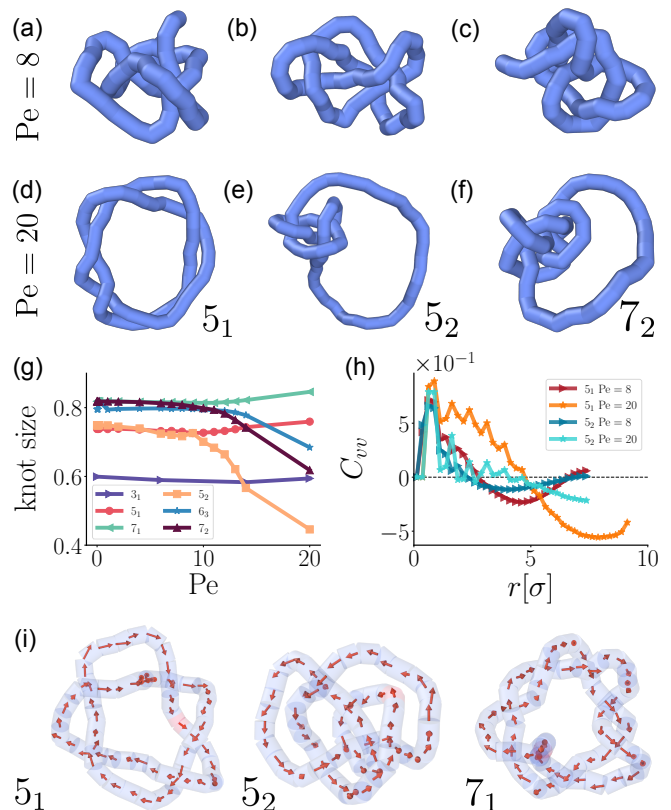


Figure 1. Localization. Activity can induce a localization or a delocalization for torus knots. (a-f) Snapshots from simulations of active knots of different knot types π , 5_1 ((a)-(d)), 5_2 ((b)-(e)) and 7_2 ((c)-(f)) at two activity strengths, $Pe = 8$ ((a)-(b)-(c)) and $Pe = 20$ ((d)-(e)-(f)). (g) Average fraction of beads in the knotted region as a function of activity for different knot types, averaged at steady state, over different replicas. (h) Beads velocity-velocity correlation function as a function of time for 5_1 and 5_2 knots simulated at low ($Pe = 8$) and high ($Pe = 20$) activity. (i) Snapshot of quasi-ideal conformation of a 5_1 , a 5_2 and a 7_2 knot from simulations at $Pe = 14$. The knots are decorated with arrows indicating the orientation of the activity.

bead velocity-velocity correlation as a function of distance in space. Correlations decay rapidly at both low and high activity for the 5_2 twist knot, while the 5_1 torus knot exhibits long-range order at sufficiently high activity. Analogous to nematic or polar ordering and phase transitions in active filament suspensions [41–43], localization and tightening of active knots represent the topological and geometric manifestations of activity-driven organization. Finally, we consider the trefoil knot 3_1 , which uniquely belongs to both torus and twist knot families. As activity varies, its knot size (Fig.1(g)) remains delocalized consistently with torus knot behavior. However, the knot size distribution is significantly broader than for pure torus or twist knots (see SI [34]), reflecting its dual topological nature.

Topology dependent persistent motion of active knots- The relationship between activity and topology not only

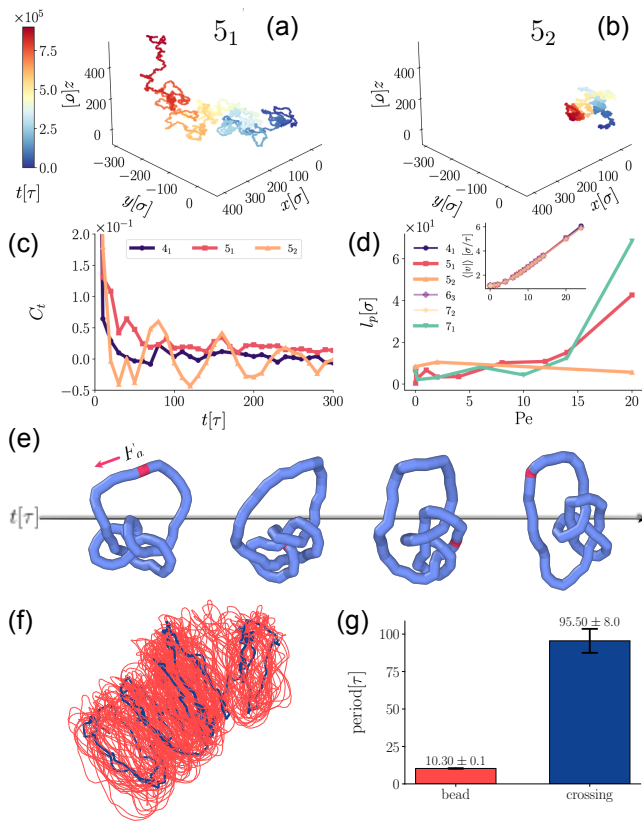


Figure 2. Persistence and reptation. (a-b) Trajectories of the center of mass of a 5_1 and a 5_2 knot simulated at $F_a = 10$. (c) Correlation function (for $Pe = 20$) and persistence length (d) of the tangents to the trajectory of the center of mass of simulated active knots. The inset in panel (d) shows the average velocity of the beads as a function of activity, for different topologies. (e) Sequence of subsequent snapshots from simulations of a 5_2 knot revolving in space. Highlighted in red is a given selected bead, which quickly traverses the whole contour before the knot shape changes significantly. (f) Trajectory of the crossing (blue) of a delocalized torus knot (5_1 for $Pe = 20$), and of one of its beads (red), over a time interval of $10^3\tau$. (g) Reptation period for the same case displayed in panel (f).

manifests through the reported conformational bias but also profoundly affects the dynamics of active knots. To probe this, we inspected the trajectories of the center of mass of the knot of various knot types for different intensities of activity. Figure 2(a,b) displays representative trajectories for 5_1 (torus) and 5_2 (twist) knots at $Pe = 20$ over equal time intervals. The torus knot 5_1 exhibits greater directional persistence than the twist knot 5_2 , resulting in larger spatial displacement. This difference in motility persistence is characterized by the trajectory tangent correlation function (Fig. 2c) and its spatial decay (or persistence) length (Fig. 2d). Note that the direction of motion is lost over a longer interval of time as the activity increases. This effect varies quantitatively with knot type: torus knots exhibit significantly larger

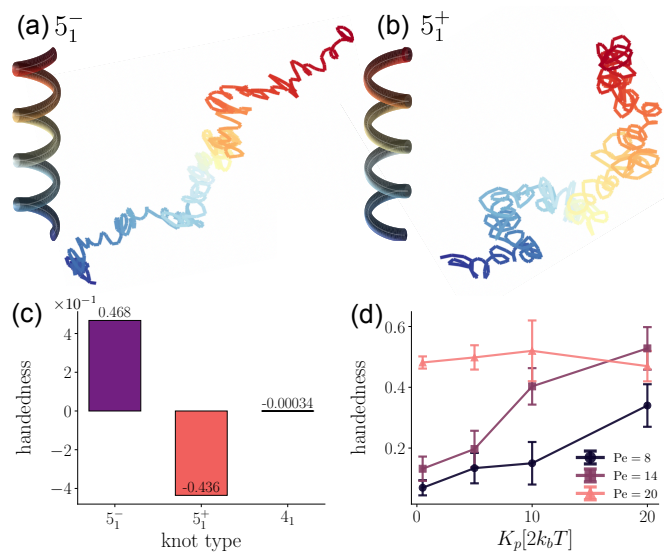


Figure 3. Chirality. (a-b) Trajectory of a crossing of a 5_1^- (a) and 5_1^+ (b) knot, over an interval of 100τ , simulated at $Pe = 20$. (c) Average handedness of the trajectories of a crossing of a simulated 5_1^- (purple), and a 5_1^+ (orange) knots, and of the trajectory of a comoving point to a simulated 4_1 knot (black bar). (d) Average handedness of comoving trajectories to 5_1^- knots simulated at $Pe = 14$ with different values of the stiffness parameter K_p .

motility persistence than other topologies, and within the torus family, higher crossing numbers yield higher persistence. Notably, enhanced persistence does not reflect local bead dynamics—Fig. 2d inset confirms that average bead velocity is topology-independent. The tangent-tangent correlation function further captures some features of the conformations of the knots: in tight knots (e.g., 5_2 at $Pe = 20$), it oscillates between parallel and antiparallel alignment, whereas it decays monotonically in all the other cases.

Another remarkable feature of the dynamics of active knots is illustrated in Fig. 2(e-f): the time it takes a bead (highlighted in red for 5_2 at $Pe = 20$) to traverse the knot is considerably shorter than the timescale over which the knot’s shape itself changes significantly. Drawing an analogy with polymer reptation in melts [44, 45], one can picture an active knot spinning within a knotted tube whose shape evolves slowly while its topology is preserved. This picture holds for all knots studied.

By tracking either the center of mass of a tight twist knot (panel 2e) or the crossings of a delocalized torus knot (red trajectory in panel 2f for 5_1 at $Pe = 20$), we observe that the knot conformation revolves in space. This reveals two distinct timescales: the reptation period (the time for a bead to complete one lap around the knot) and the knot’s revolution period. These timescales are reported in Fig. 2g for the same case as panel (f). The revolution period of the crossing trajectory is a factor of 10 larger than the reptation period of the bead, implying that the bead traverses the knot 10 times per knot

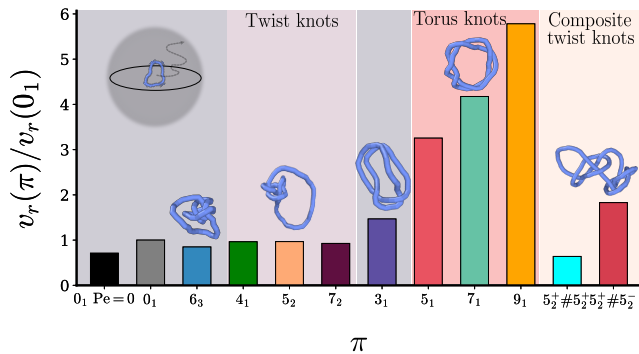


Figure 4. **Topology and efficiency.** Average radial velocity for various knot types π relative to the unknot (0_1) at $Pe = 20$. As shown in the top-left inset, this is calculated from the first passage time out of a spherical boundary of radius $r = 25\sigma$. For comparison, the result for the unknots at $Pe = 0$ is reported too (black bar). Note that the composite knots are twice as long ($N_b = 128$) and stiffer ($K_p = 10k_bT$) than the prime knots.

revolution.

Dynamic chirality in active knots- Having explored how topology and activity interplay to create distinct conformational and dynamical regimes, we now turn to another fundamental topological feature of an active knot, namely its chirality. Most knot types cannot be continuously deformed into their mirror images and thus exist in left-handed ($-$) and right-handed ($+$) forms. Exceptions are achiral (or amphichiral) knots, whose mirror images are topologically equivalent. Of the knots considered here, 4_1 and 6_3 are achiral, while all others are chiral. Inspecting the trajectories of the knots by chirality reveals that this property reverberates through their dynamics as follows. As described previously, delocalized torus knots and localized twist knots revolve around their center of mass, which maintains a fixed spatial direction for times increasing with activity. Consequently, a point rigidly attached to the knot shape, such as a crossing in a highly active torus knot, traces a spiral trajectory in space, as illustrated in Fig. 3(a-b). Strikingly, spiral motions driven by 5_1^- and 5_1^+ knots display definite but opposite chirality (panels 3a and 3b). We quantify this observation by computing a local handedness $h(t)$ at each trajectory point. Following the procedure detailed in the SI [34], we associate a triad of vectors describing how the crossing trajectory bends relative to the center-of-mass trajectory. The scalar triple product of this triad yields $h(t) = +1$ for right-handed and $h(t) = -1$ for left-handed configurations. The average handedness of the trajectory of the crossings [34] of 5_1^+ and 5_1^- knots is reported in Fig. 3c for $Pe = 20$ (orange and purple bars, respectively) and indicates that the left-handed 5_1^- follows a predominantly right-handed trajectory, whereas the right-handed 5_1^+ knots exhibit the opposite trend. This behavior is reminiscent of chirality-dependent sedimentation observed in 3D-printed knots [46, 47]. Here,

however, persistent self-propulsion emerges from the interplay of topology, activity, and chirality.

We also analyzed achiral 4_1 knot trajectories at $Pe = 20$. Because 4_1 conformations deviate significantly from quasi-flat geometries, resolving their crossings is difficult. Decoupling the knot's shape trajectory from high-frequency individual bead rotation thus requires a more general approach. As detailed in the SI, we characterize shape evolution by identifying comoving trajectories, namely time sequences of beads that move alongside the knot image. The 4_1 knot fails to maintain persistent chirality, showing near-zero net handedness (Fig. 3(c), black bar).

To understand how baseline rigidity affects handedness and trajectory persistence, we varied the stiffness parameter K_p at different activity values. Results for a 5_1^- knot at $Pe = 20, 14$ and 8 are shown in Fig. 3(d). As K_p increases and the knot inflates toward ideal conformations, trajectory handedness stabilizes. This stabilization is more pronounced at lower activity since activity itself enhances effective knot stiffness.

Finally, to emphasize how topology influences the self-propulsion efficiency of soft rings, we measured the escape rate of various active knots from a spherical boundary, normalized by the unknot's rate. The results in Fig. 4 show that torus knots are the most efficient self-propellers. Their escape speed increases nearly linearly with crossing number, with the 9_1 knot escaping approximately six times faster than the unknot.

Discussion and conclusions- In conclusion, we have shown that the physics of active polymer knots is fundamentally determined by their topology. Torus and twist knots behave asymmetrically: while twist knots localize along the ring, torus knots generically delocalize under activity. This behavior contrasts with passive polymers under tension, where knots typically tighten and localize. We attribute this difference to the distinct internal organization of the two families: torus knots exhibit higher polar alignment of active segments, promoting cooperative propulsion along the backbone and spreading of the knotted region, whereas twist knot geometry disrupts this alignment and stabilizes a compact core.

Activity also enables spontaneous self-assembly of a topological persistent chiral rotor, where the knotted region acts as a soft quasiparticle driving persistent motion of the entire ring. The resulting trajectories display biomimetic helical motility similar to that observed in active filaments and microorganisms [31], with persistence strongly dependent on topology: torus knots generate highly persistent chiral motion, while unknotted rings or twist knots display significantly less persistent trajectories. Together, these results demonstrate that polymer topology can program the transport properties and dynamical organization of active polymers.

These findings suggest several directions for future work. An important question concerns the collective behavior of active knot melts, where topology may govern emergent phases and transport—analogueous to active

topological glasses formed by unknotted rings [17]. Another interesting extension is that of electrophoretic motility of active DNA knots, where it would be interesting to see whether the topology-dependent persistence translates into differential mobilities. Finally, activity may

enable interactions between multiple knots on the same chain, potentially creating novel nonequilibrium topological states worth characterizing. More broadly, our results suggest that active knots represent a new class of topological soft matter, where knotted regions act as self-organized active quasiparticles with tunable properties.

-
- [1] B. Alberts, D. Bray, K. Hopkin, A. D. Johnson, J. Lewis, M. Raff, K. Roberts, and P. Walter, *Essential cell biology* (Garland science, 2015).
- [2] S. A. Sevier and H. Levine, Properties of gene expression and chromatin structure with mechanically regulated elongation, *Nucleic acids research* **46**, 5924 (2018).
- [3] G. Forte, C. A. Brackley, N. Gilbert, and D. Marenduzzo, Nonequilibrium polymer models for chromatin, *Curr. Opin. Genet. Devel.* **96**, 102426 (2026).
- [4] E. Alipour and J. F. Marko, Self-organization of domain structures by dna-loop-extruding enzymes, *Nucleic acids research* **40**, 11202 (2012).
- [5] A. D. Bates and A. Maxwell, *DNA topology* (Oxford University Press, USA, 2005).
- [6] A. Zidovska, D. A. Weitz, and T. J. Mitchison, Micron-scale coherence in interphase chromatin dynamics, *Proceedings of the National Academy of Sciences* **110**, 15555 (2013).
- [7] V. Bianco, E. Locatelli, and P. Maggaretti, Globulelike conformation and enhanced diffusion of active polymers, *Phys. Rev. Lett.* **121**, 217802 (2018).
- [8] M. Fogliano, E. Locatelli, C. Brackley, D. Michieletto, C. Likos, and D. Marenduzzo, Non-equilibrium effects of molecular motors on polymers, *Soft Matter* **15**, 5995 (2019).
- [9] R. G. Winkler, J. Elgeti, and G. Gompper, Active polymers—emergent conformational and dynamical properties: A brief review, *J. Phys. Soc. Jpn.* **86**, 101014 (2017).
- [10] G. Zhu, L. Gao, Y. Sun, W. Wei, and L.-T. Yan, Non-equilibrium structural and dynamic behaviors of active polymers in complex and crowded environments, *Reports on Progress in Physics* **87**, 054601 (2024).
- [11] T. Sakaue and E. Carlon, Physics of active polymers: scaling analysis via a compounding formula, arXiv:2603.05652 (2026).
- [12] D. Breoni, E. Locatelli, and L. Tubiana, Effects of knotting on the collapse of active ring polymers, *Macromolecules* **58**, 10677 (2025).
- [13] M. Vatin, E. Orlandini, and E. Locatelli, Upsurge of spontaneous knotting in polar diblock active polymers, *Physical Review Letters* **134**, 168301 (2025).
- [14] J. P. Miranda, E. Locatelli, and C. Valeriani, Self-organized states from solutions of active ring polymers in bulk and under confinement, *J. Chem. Theory Comput.* **20**, 1636 (2023).
- [15] A. Lamura, Excluded volume effects on tangentially driven active ring polymers, *Phys. Rev. E* **109**, 054611 (2024).
- [16] J. Prost, F. Jülicher, and J.-F. Joanny, Active gel physics, *Nature physics* **11**, 111 (2015).
- [17] J. Smrek, I. Chubak, C. N. Likos, and K. Kremer, Active topological glass, *Nat. Commun.* **11**, 26 (2020).
- [18] C. Micheletti, I. Chubak, E. Orlandini, and J. Smrek, Topology-based detection and tracking of deadlocks reveal aging of active ring melts, *ACS macro letters* **13**, 124 (2024).
- [19] C. N. Likos, Soft matter with soft particles, *Soft Matter* **2**, 478 (2006).
- [20] R. Metzler, W. Reisner, R. Riehn, R. Austin, J. Tegenfeldt, and I. M. Sokolov, Diffusion mechanisms of localised knots along a polymer, *EPL* **76**, 696 (2006).
- [21] B. Marcone, E. Orlandini, A. Stella, and F. Zonta, What is the length of a knot in a polymer?, *J. Phys. A* **38**, L15 (2005).
- [22] O. Farago, Y. Kantor, and M. Kardar, Pulling knotted polymers, *EPL (Europhysics Letters)* **60**, 53 (2002).
- [23] M. Caraglio, C. Micheletti, and E. Orlandini, Stretching response of knotted and unknotted polymer chains, *Physical review letters* **115**, 188301 (2015).
- [24] C. B. Renner and P. S. Doyle, Untying knotted dna with elongational flows, *ACS Macro Letters* **3**, 963 (2014).
- [25] C. C. Adams, *The Knot Book* (Freeman, 1994).
- [26] B. Liebchen, M. E. Cates, and D. Marenduzzo, Pattern formation in chemically interacting active rotors with self-propulsion, *Soft Matter* **12**, 7259 (2016).
- [27] B. Liebchen and D. Levis, Collective behavior of chiral active matter: Pattern formation and enhanced flocking, *Phys. Rev. Lett.* **119**, 058002 (2017).
- [28] L. Caprini, B. Liebchen, and H. Löwen, Self-reverting vortices in chiral active matter, *Commun. Phys.* **7**, 153 (2024).
- [29] Y. Arai, R. Yasuda, K.-i. Akashi, Y. Harada, H. Miyata, K. Kinoshita Jr, and H. Itoh, Tying a molecular knot with optical tweezers, *Nature* **399**, 446 (1999).
- [30] X. R. Bao, H. J. Lee, and S. R. Quake, Behavior of complex knots in single dna molecules, *Physical review letters* **91**, 265506 (2003).
- [31] L. N. Carenza, G. Gonnella, D. Marenduzzo, and G. Negro, Rotation and propulsion in 3d active chiral droplets, *Proc. Natl. Acad. Sci. USA* **116**, 22065 (2019).
- [32] L. Carenza, G. Gonnella, D. Marenduzzo, and G. Negro, Chaotic and periodical dynamics of active chiral droplets, *Physica A: Statistical Mechanics and its Applications* **559**, 125025 (2020).
- [33] S. Plimpton, Fast parallel algorithms for short-range molecular dynamics, *Journal of Computational Physics* **117**, 1 (1995).
- [34] Supplemental Material available at xxx.
- [35] L. Tubiana, G. Polles, E. Orlandini, and C. Micheletti, Kymoknot: A web server and software package to identify and locate knots in trajectories of linear or circular polymers, *The European Physical Journal E* **41**, 72 (2018).
- [36] L. Tubiana, E. Orlandini, and C. Micheletti, Probing the entanglement and locating knots in ring polymers: a comparative study of different arc closure schemes,

- Progress of Theoretical Physics Supplement **191**, 192 (2011).
- [37] V. Katritch, J. Bednar, D. Michoud, R. G. Scharein, J. Dubochet, and A. Stasiak, Geometry and physics of knots, *Nature* **384**, 142 (1996).
- [38] E. Orlandini, M. C. Tesi, E. J. Van Rensburg, and S. G. Whittington, Asymptotics of knotted lattice polygons, *Journal of Physics A: Mathematical and General* **31**, 5953 (1998).
- [39] A. Bonato, E. Orlandini, and S. Whittington, Asymptotics of linked polygons, *Journal of Physics A: Mathematical and Theoretical* **53**, 385002 (2020).
- [40] A. Bonato, E. Orlandini, and S. Whittington, Asymptotics of multicomponent linked polygons, *Journal of Physics A: Mathematical and Theoretical* **54**, 235002 (2021).
- [41] A. Joshi, E. Putzig, A. Baskaran, and M. F. Hagan, The interplay between activity and filament flexibility determines the emergent properties of active nematics, *Soft Matter* **15**, 94 (2019).
- [42] M. G. Athani and D. A. Beller, Symmetry and stability of orientationally ordered collective motions of self-propelled, semiflexible filaments, *Phys. Rev. Res.* **6**, 023319 (2024).
- [43] J. P. Miranda-Lopez, E. Locatelli, C. Micheletti, D. Levis, and C. Valeriani, Geometrical entanglement and alignment regulate self-organization in active ring polymer suspensions, *Journal of Chemical Theory and Computation* **21**, 11910 (2025).
- [44] P. G. de Gennes, Reptation of a polymer chain in the presence of fixed obstacles, *The Journal of Chemical Physics* **55**, 572 (1971).
- [45] M. Doi and S. F. Edwards, Dynamics of concentrated polymer systems. part 1.—brownian motion in the equilibrium state, *J. Chem. Soc., Faraday Trans. 2* **74**, 1789 (1978).
- [46] C. Weber, M. Carlen, G. Dietler, E. J. Rawdon, and A. Stasiak, Sedimentation of macroscopic rigid knots and its relation to gel electrophoretic mobility of dna knots, *Scientific Reports* **3**, 1091 (2013).
- [47] M. Gruzziel, K. Thyagarajan, G. Dietler, A. Stasiak, M. L. Ekiel-Jezewska, and P. Szymczak, Periodic motion of sedimenting flexible knots, *Phys. Rev. Lett.* **121**, 127801 (2018).